

# Deformation and Dissipated Energy of Sandstone Under Uniaxial Cyclic Loading

Huiqiang Duan · Yongjie Yang

Received: 16 February 2017 / Accepted: 15 July 2017 / Published online: 20 July 2017  
© Springer International Publishing AG 2017

**Abstract** The fatigue deformation of sandstone was investigated in the laboratory using uniaxial cyclic loading tests. These tests showed that: (1) Fatigue deformation can be divided into three phases, the primary, steady, and acceleration phases. The initiation of the acceleration phase indicates that the sample is about to fail. (2) Sandstone samples subjected to conventional compression tests fail in a different way than samples subjected to cyclic loading tests. The former mainly fail along shear and tensile fractures whereas the latter are transformed into a pile of many large and small fragments. (3) When sandstone is undergoing cyclic loading, the extent of deformation and the dissipated energy change synchronously, so the energy dissipation curve can reflect the fatigue deformation of the sandstone. (4) A model for sandstones deformed by cyclic loading is put forward that describes the U-shaped distribution of energy dissipation points on an energy dissipation-cycle number plot well.

**Keywords** Cyclic loading · Deformation · Failure mode · U-shaped dissipated energy evolution model

## 1 Introduction

In underground mines, in addition to the static loading, the rock is also affected by cyclic loading caused by the mining itself. In many cases, the deformation and instability of the rock surrounding underground roadways is mainly caused by this cyclic loading. Therefore, the study of the fatigue in rock masses under cyclic loading is very important and the research findings from such studies can be used to evaluate the stability of rock masses and thereby contribute to preventing dynamic mine disasters and accidents. This would promote mine safety and ensure safe production.

Many researchers have studied rock fatigue. For example, studies have shown that the fatigue failure of rock is controlled by the static stress–strain curve and that the axial residual strain can be divided into three phases: the primary, steady, and acceleration phases (Ge et al. 2003; Zhang et al. 2006; Lu et al. 2015, 2016). Some researchers have studied the different factors influencing rock fatigue. These research findings have shown that the peak stress, amplitude, loading frequency, and initial stress of cyclic loading have a significant influence on the rock's fatigue failure (Feng et al. 2009; Fuenkajorn and Phueakphum 2010; Yang et al. 2007; Hamid and Abdolhadi 2014; Araei et al. 2012; He et al. 2016; Jiang et al. 2016; Bagde et al. 2005, 2009). Some authors have reported on the energy dissipated by rocks subjected to cyclic loading. For example during

---

H. Duan (✉) · Y. Yang  
College of Mining and Safety Engineering, Shandong  
University of Science and Technology,  
Qingdao 266590, Shandong, China  
e-mail: duanhuiqiang11@163.com

experiments on sandstone, He et al. (2015) found that both axial strain and energy dissipation evolve through three phases when the peak stress of cyclic loading exceeded the fatigue strength of the sandstone.

This paper investigates the fatigue of sandstone under cyclic uniaxial loading because sandstone beds are present in many mines.

## 2 Experimental Methods

### 2.1 Test Equipment

Tests were conducted using an MTS815.02 rock mechanics test system (MTS Systems Corporation, Eden Prairie, MN, U.S.A.). Compared with some other rock mechanics test systems, the MTS815.02 system has the following advantages. (1) The test machine is constructed with a solid steel body and only a small amount of elastic energy is stored during testing. This means a rigorous pressure test can be conducted. (2) The strain can be accurately measured using an extensometer from American MTS Systems Corporation (a patented product). (3) The test system is very stable.

### 2.2 Samples Tested

The sandstone samples were collected from a fluvial sandstone in a coal mine in Shandong Province, China. The cylindrical samples were approximately 100 mm long and 50 mm in diameter. The samples selected for the tests had no cracks or joints.

### 2.3 Test Procedures

Two types of tests were performed, conventional uniaxial compression tests and cyclic uniaxial loading tests. Conventional uniaxial compression tests were carried out using the displacement-control mode. The aim of the testing was to obtain complete stress–strain curves and determine the strength of the sandstone samples to provide essential data for the cyclic loading tests. Previous research has shown that the peak strength of a rock as determined by conventional compression tests increases with an increase in the loading rate (Wu 1982). However if the loading rate is less than a specific threshold, the loading rate has very little influence on the rock's strength. The strain loading rate threshold is  $10^{-4}$ /s (Yin et al. 2010),

therefore the strain loading rate should not exceed 0.01 mm/s when the sample length is 100 mm. In this paper, the strain loading rate for the conventional uniaxial compression tests was 0.003 mm/s.

Cyclic uniaxial loading tests were performed under the stress-control mode in which loading stops when the axial displacement of the sample exceeds 3 mm. Prior to each test, an initial force of 1.0 kN was applied to ensure close contact between the test machine's piston head and the sample. The linear loading rate was 0.2 kN/s. Each sample was deformed with a cosine waveform at a frequency of 0.25 Hz. The axial valley stress and peak stress were fixed. The loading path for a cyclic loading test is shown in Fig. 1.

## 3 Test Results

Three samples were selected for conventional uniaxial compression test. The peak strengths of these samples were 53.07, 62.25, and 57.69 MPa; their average strength was 57.67 MPa. The test results showed that there was considerable variation in the strength of the samples. Figure 2 shows the stress–strain curves for those three samples.

### 3.1 Deformation and Fatigue Failure

Table 1 lists test results for the three samples subjected to cyclic loading tests. Figure 3a, b compare the axial stress–strain curves for the cyclic loading and the conventional uniaxial compression tests. It is quite clear that there is little difference in failure

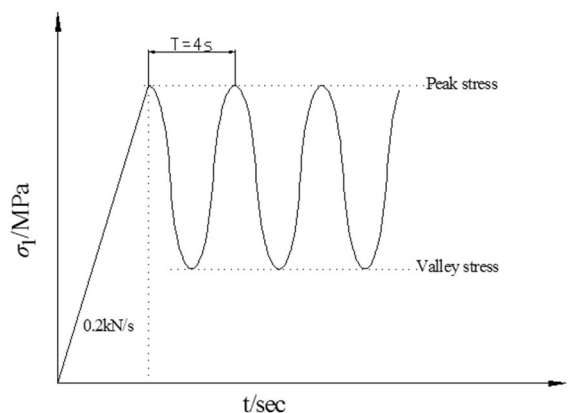


**Fig. 1** The Loading path in cyclic loading test

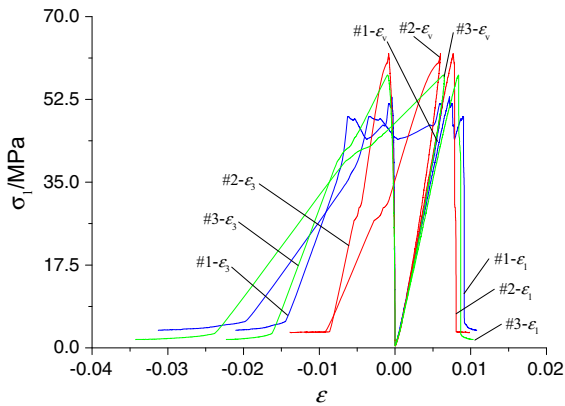


**Fig. 2** Stress–strain curves for sandstone samples from conventional uniaxial compression tests. The symbols  $\sigma_1$ ,  $\epsilon_1$ ,  $\epsilon_3$ , and  $\epsilon_v$  signify the axial stress, axial strain, circumferential strain, and volumetric strain, respectively

deformation between samples deformed by cyclic loading tests and those deformed by uniaxial compression tests.

### 3.2 The Three Phases of Fatigue

The axial fatigue curves for rock take three forms depending on the relationship between peak cyclic loading stress and the fatigue strength of the sample. These three forms are shown in Fig. 4 (Ge et al. 2003).

When the peak stress of cyclic loading is less than the fatigue strength of the sample, the shape of the fatigue curve is that of curve “a” in Fig. 4 and the sample deformation does not increase after a certain number of cycles. When the peak stress of cyclic loading is slightly higher than the fatigue strength of the sample, the shape of the fatigue curve becomes that shown by curve “b” in Fig. 4. The fatigue undergone by samples of this type can be divided into three phases, primary, steady, and acceleration phases. The third type of fatigue curve, curve “c” in Fig. 4, is produced when the peak stress of cyclic loading is close to the peak strength of the sample. In this situation, the fatigue curve is approximately linear and the sample will fail after only a few cycles.

Figure 5a, b, c show the curves for axial, circumferential, and volumetric strains versus cycle number for the three samples tested. The strain after failure is not shown.

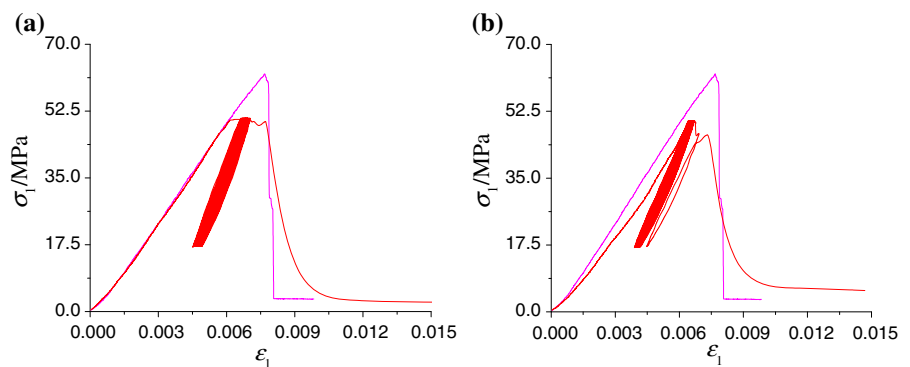
The fatigue curves in Fig. 5a are curves of type “c” as shown in Fig. 4. For the first 35 cycles, the fatigue curves are approximately linear. After cycle number 35, the strain rate increase and sample deformation falls into the acceleration deformation phase.

The fatigue curves in Fig. 5b are type “b” curves as shown in Fig. 4. For the first five cycles, the fatigue is in the primary phase. Between 6 and 60 cycles, the

**Table 1** Test conditions and results for three samples tested under cyclic uniaxial loading

Sample number	Loading Frequency/(Hz)	Valley stress/(MPa)	Peak stress/(MPa)	Stress amplitude/(MPa)	Cyclic number	Failure state
1#	0.25	17.3	50.2	32.9	38	Failed
2#	0.25	17.3	49.7	32.4	63	Failed
3#	0.25	17.3	50.0	32.7	2400+	Not failed

**Fig. 3** Comparison of axial stress–strain curves for samples tested by cyclic loading and conventional uniaxial compression tests. **a** Sample #1, **b** sample #2



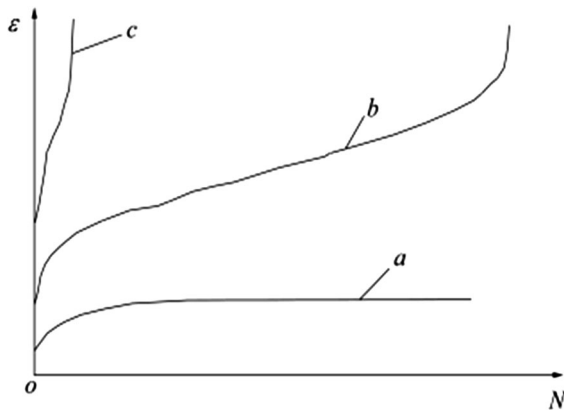


**Fig. 4** Diagrammatic sketch showing fatigue curves for rocks with different relationships between peak cyclic loading stress and the sample's fatigue strength (from Ge et al. 2003)

fatigue in the steady phase and after 60 cycles, the fatigue in the acceleration phase.

The fatigue curves in Fig. 5c are type “a” as shown in Fig. 4. For the first 500 cycles, the strain increases at a decreasing rate as the cycle number increases and the fatigue is in the primary phase. After 500 cycles, the strain increases at an almost constant rate with increasing cycle number, indicating that the fatigue is in the steady phase.

The test results shown that the axial, circumferential, and volumetric strains in the sample increase simultaneously near the end of the acceleration phase. The behavior indicates that the sample is about to fail.

It is important to point out that the steady phase of sandstone deformation actually means that the resid-

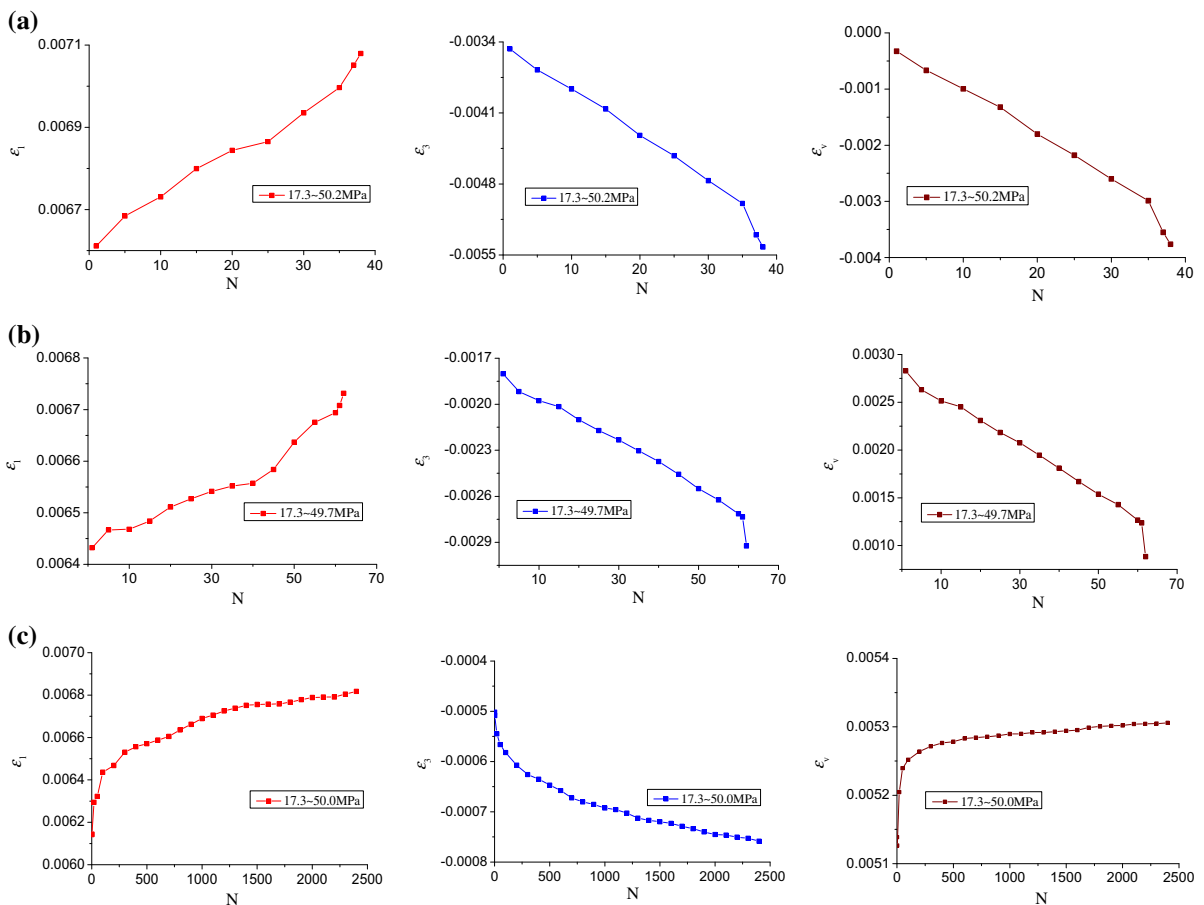
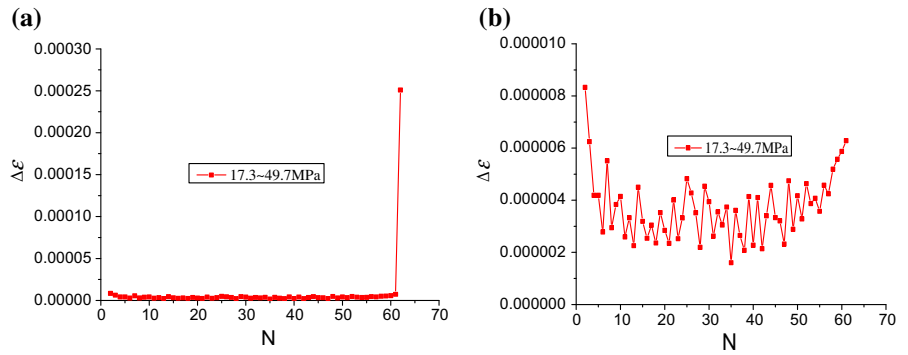


**Fig. 5** Graphs showing the relationships between axial ( $\epsilon_1$ ), circumferential ( $\epsilon_3$ ), and volumetric ( $\epsilon_v$ ) strains and cycle number (N) for the three samples tested by cyclic uniaxial loading. **a** Sample #1, **b** sample #2, **c** sample #3

**Fig. 6** Graphs showing axial residual strain versus cycle number for sample #2. Panels 6a and 6b show the same data but with different Y-axis scales. **a** Cycles 2–62, **b** cycles 2–61



ual strain in each cycle fluctuates within a range. The axial residual strain versus cycle number for sample #2 reflects this fact, as shown in Fig. 6.

### 3.3 Sample Failure

Figure 7 presents photographs showing sandstone samples after failure. The samples shown in Fig. 7a failed after being compressed by conventional uniaxial compression tests whereas the samples in Fig. 7b failed after cyclic loading compression tests.

The conventionally compressed samples mainly failed along shear and tensile fractures, however failure transformed the cyclically loaded samples into several large blocks and numerous smaller fragments. The difference in failure mode is the result of different crack propagation mechanisms. During a conventional uniaxial compression test, the micro defects in the sample cannot develop fully because the time required for the test is very short. Most of the axial mechanical

energy imparted by the test machine is consumed by several large cracks that finally cause failure. During a cyclic loading test, the micro cracks in the sample can develop fully because the time required for the test is much longer. In addition, the propagation of large cracks is restricted during cyclic loading because the peak stress of cyclic loading is lower than the peak strength of the sample. Most of the mechanical energy imparted by test machine is consumed by the many micro cracks in sample. The abundant, propagating micro cracks are the reason the sample finally fails and breaks into numerous pieces.

## 4 Discussion and Energy Dissipation

### 4.1 Dissipated Energy Calculations

The deformation and failure of rock are closely related to energy transfer. Where energy is transferred during

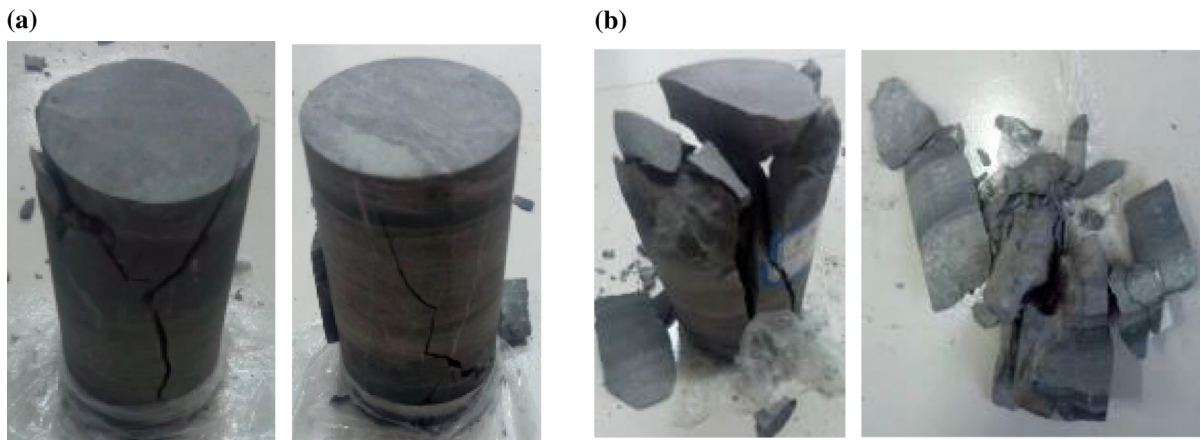


**Fig. 7** Photographs showing the different failure modes for samples compressed by conventional uniaxial compression and cyclic uniaxial loading tests **a** Conventional uniaxial compression test failure **b** Cyclic loading compression test failure

rock deformation can reflect the damage to the rock (Ma 2016). During compression tests, some of the energy forced into the rock is stored in the form of elastic strain energy and the rest, called dissipation energy, is dissipated in the form of heat and radiation (He et al. 2015 and Lazan. 1968).

The area of the hysteresis loop in the rock's stress–strain curve under cyclic loading has been used by some workers to represent the magnitude of the dissipated energy (Bagde and Petroš 2009; Xiao et al. 2010).

The area of the axial hysteresis loop is the difference between the area under the loading curve and the area under the unloading curve (Zhang 2011). The calculation for the area of the axial hysteresis loop used in this paper is illustrated in the example below.

In Fig. 8, the area under the axial loading curve (area ABCD) is the unit volume energy for a loading–unloading cycle, expressed as  $U_+$ . The area under the axial unloading curve (area A'B'CD) is the elastic strain energy per unit volume for a loading–unloading cycle, expressed as  $U_-$ . Because  $U_+$  is positive and  $U_-$  is negative, the sum of the two is the dissipated energy per unit volume,  $U$ . The “ $U$ ” value can be obtained by integrating the trapezoidal areas shown in Fig. 8. The relationship between  $U$ ,  $U_+$ , and  $U_-$  is (Zhang 2011):

$$U = U_+ + U_-$$

$$= \sum_{i=1}^n (\sigma_{1,i} + \sigma_{1,i+1}) \cdot (\varepsilon_{1,i+1} - \varepsilon_{1,i}) / 2 \quad (1)$$

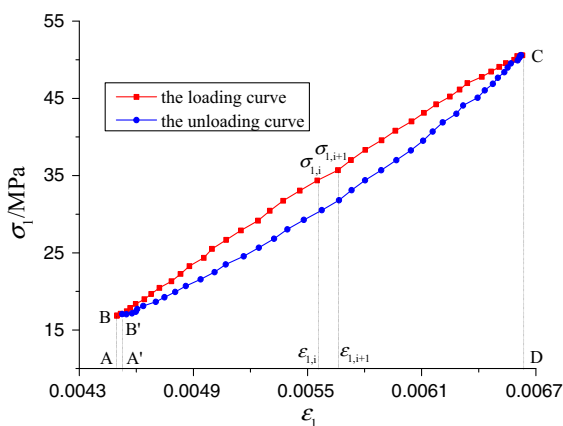


**Fig. 8** Graph illustrating the method for calculating the area of the hysteresis loop

## 4.2 Dissipated Energy and Compression Cycles

The hysteresis loop in the first compression cycle is not representative because the stress was linearly loaded and unloaded in a cosine waveform. As explained below, the hysteresis loop for the last compression cycle is also not representative. Figure 9 illustrates the stress–strain curves for the 37th and 38th compression cycles for sample #1, the sample that failed at cycle #38 (Table 1). In Fig. 9, point “a” is defined as the failure point (Ge et al. 2003).

From point “a” on, the maximum peak stress in each cycle cannot rise to the designed peak stress for that cycle's load. For this reason, the hysteresis loops at or after the failure point are also not representative. Through analysis of these stress–strain curves, it was found that cycles 2 through 37, for sample #1, and cycles 2 through 61 for sample #2 (which lost all of its carrying capacity at cycle #63) were normal loading–unloading cycles with the same peak and valley stresses for those samples.

In Figs. 10, 11, the dissipated energy per unit volume versus cycle number curves are approximately U-shaped and can be divided into three phases, the primary, steady, and acceleration phases. In Fig. 12, the dissipated energy per unit volume versus cycle number curve is approximately L-shaped and can be divided into two phases, the primary and steady phases.

In general, the deformation of rock is closely related to energy dissipation and the larger the axial residual strain in a cycle, the larger the amount of

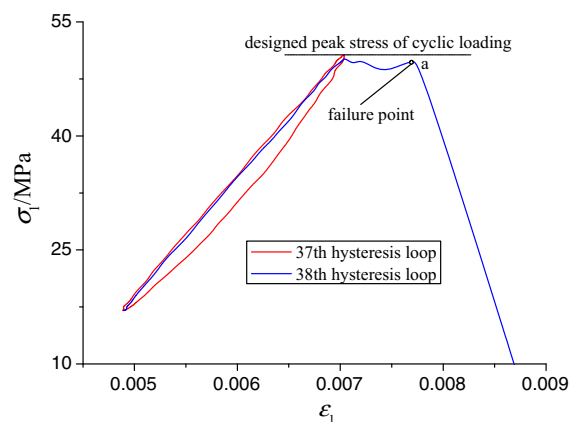


**Fig. 9** Stress–strain curves for the 37th and 38th compression cycles for sample #1 showing the failure point “a”

**Fig. 10** Graphs showing dissipated energy per unit volume versus cycle number for sample #1. Panels 10a and 10b show the same data but with different Y-axis scales **a** Cycles 1–38 **b** Cycles 2–37

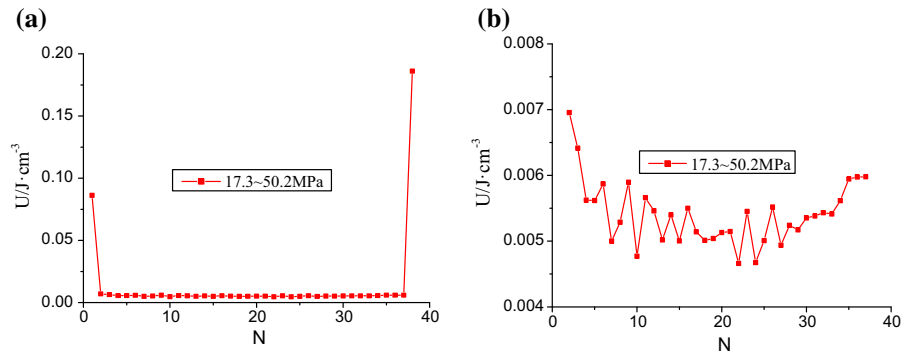


**Fig. 11** Graphs showing dissipated energy per unit volume versus cycle number for sample #2. Panels 11a and 11b show the same data but with different Y-axis scales **a** Cycles 1–63 **b** Cycles 2–61

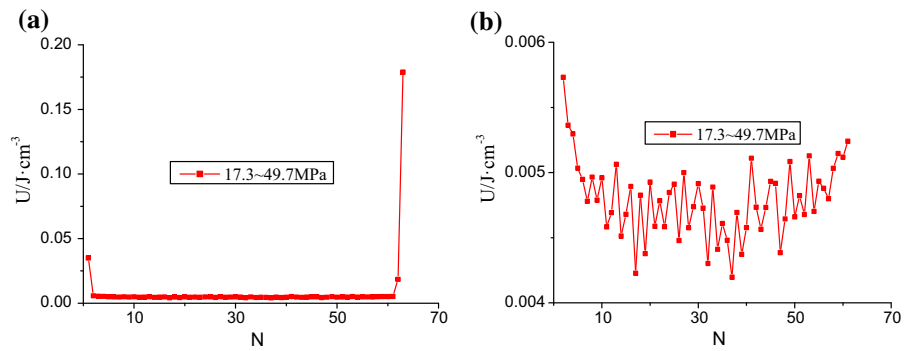
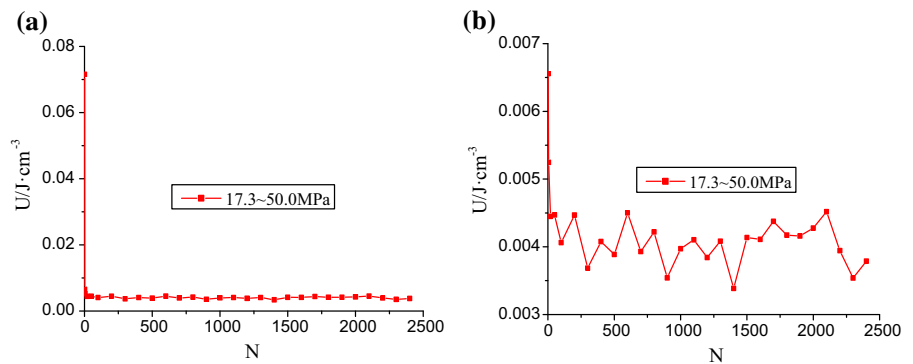


**Fig. 12** Graphs showing dissipated energy per unit volume versus cycle number for sample #3. Panels 12a and 12b show the same data but with different Y-axis scales **a** Cycles 1–2400 **b** Cycles 2–2400



dissipated energy. In the primary phase, both the dissipated energy and the residual strain gradually decrease with increasing cycle number. In the steady phase, the dissipated energy fluctuates in a small range as the cycle number increases, indicating that the cumulative residual strain is increasing at an almost constant rate. In the acceleration phase, both the dissipated energy and the residual strain increase rapidly at an increasing rate with increasing cycle number. For these reasons, the energy dissipation curve can also reflect the fatigue evolution of the rock.

### 4.3 A Model for Dissipated Energy

He et al. (2015) found that the relationship between dissipated energy and stress amplitude is exponential and gave the following equation:

$$U(\Delta\sigma, N) = aN^b(\Delta\sigma)^{cNd} \tag{2}$$

where U is dissipated energy; N is the cycle number, and a, b, c, and d are parameters concerning rock properties.

Equation (2) can only describe the L-shaped curve for dissipated energy versus cycle number and the equation cannot be applied to the U-shaped curves. In general,



**Fig. 13** Graphs showing curves fit to the dissipated energy data for samples #1 **a** and #2 **b** when the “Y” in Eq. (3) is a second order polynomial **a** Sample #1 **b** Sample #2

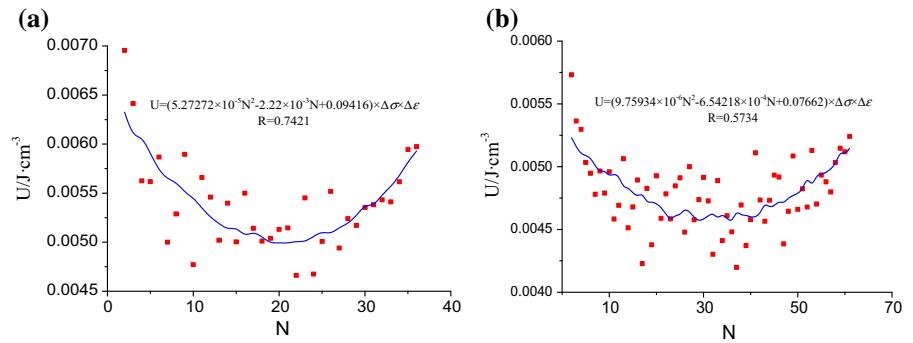
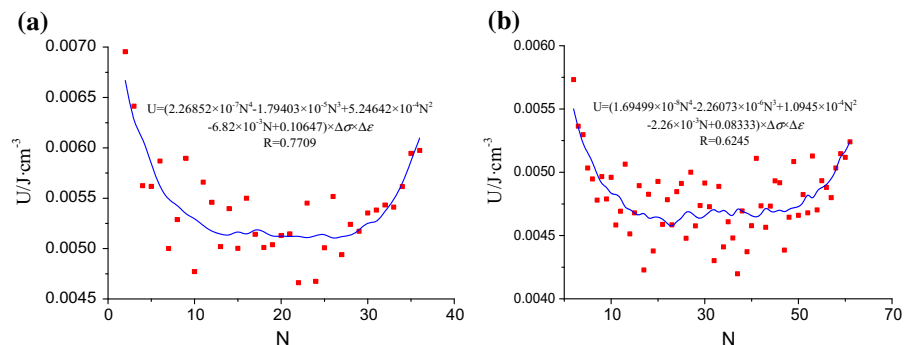


**Fig. 14** Graphs showing curves fit to the dissipated energy data for samples #1 **a** and #2 **b** when the “Y” in Eq. (3) is a fourth order polynomial **a** Sample #1 **b** Sample #2



whether linear, logarithmic, or exponential and power function and their combined forms are used, the fit to U-shaped dissipated energy versus cycle number curves would be very poor. The following two methods can be used to fit U-shaped curves. (1) First divide the whole curve into segments according to the shape of the curve. Then choose a proper function to fit each segment. (2) Use a polynomial function to fit the whole curve.

Using the first method results in a very bad fit no matter what kind of equations are used for each segment because there is considerable variation in the amplitude of the sample’s dissipated energy. However, a polynomial function can be used to great advantage for fitting complex curves. Thus the following energy dissipation model is proposed:

$$U = Y \times \Delta\sigma \times \Delta\varepsilon \quad (3)$$

where  $U$  is the dissipated energy amplitude in a cycle and  $Y$  is a polynomial function whose order should be greater than or equal to two. The general form of the appropriate quadratic polynomial equation is  $Y = aN^2 + bN + c$  where  $a$ ,  $b$ , and  $c$  are fitting coefficients and  $\Delta\sigma$  and  $\Delta\varepsilon$  are the axial stress amplitude and the axial strain amplitude in a cycle, respectively.

Origin8.6 data analysis and graphing software (OriginLab Corp, Northampton, MA, USA) allows user to define multivariable functions and perform multivariate fitting. For this paper, the fitting and analysis were both done using Origin.

Curves fit to the data for samples #1 and #2 when the  $Y$  in Eq. (3) is a quadratic polynomial are shown in Fig. 13. The correlation coefficients for samples #1 and #2 were 0.7421 and 0.5734, respectively. When the  $Y$  in Eq. (3) is a fourth order polynomial, the corresponding fitting curves, shown in Fig. 14, have correlation coefficients for the two samples of 0.7709 and 0.6245. It is quite clear that the correlation coefficient increases when  $Y$  is a higher order polynomial.

## 5 Conclusions

1. Fatigue evolution can be divided into three phases, the primary, steady, and acceleration phases. In the primary phase, the axial, circumferential, and volumetric strains in the sample increase with increasing cycle number at a decreasing rate. In the steady phase, the strains



increase with cycle number at an almost constant rate. In the acceleration phase, the strains increase with cycle number at an increasing rate. The initiation of the acceleration phase indicates that the sample is about to fail.

2. Sandstone samples compressed by conventional uniaxial compression and samples compressed by cyclic loading fail in very different ways. The conventionally compressed samples mainly fail along shear and tensile fractures but remain standing whereas the cyclically compressed samples are transformed into a pile composed of many large and small fragments.
3. When sandstone is undergoing cyclic loading, the extent of deformation and the dissipated energy change synchronously so the energy dissipation curve can also reflect the fatigue deformation of the sandstone.
4. A model for sandstones deformed by cyclic loading is put forward that describes the U-shaped distribution of energy dissipation points on an energy dissipation-cycle number plot well.

**Acknowledgements** This research was supported by the National Natural Science Foundation of China (Grant Nos. 51379116 and 51574156), and the Natural Science Foundation of Shandong Province of China (Grant No. ZR2013EEZ001). We thank David Frishman, PhD, from Edanz Group China ([www.liwenbianji.cn/ac](http://www.liwenbianji.cn/ac)) for editing the English text of a draft of this manuscript.

## References

- Araei AA, Razeghi HR, Ghalandarzadeh A (2012) Effects of loading rate and initial stress state on stress-strain behavior of rock fill materials under monotonic and cyclic loading condition. *Scientia Iranica* 9(15):1220–1235
- Bagde MN, Petroš V (2005) Fatigue properties of intact sandstone samples subjected to dynamic uniaxial cyclical loading. *Int J Rock Mech Min Sci* 42(2):237–250
- Bagde MN, Petroš V (2009) Fatigue and dynamic energy behavior of rock subjected to cyclical loading. *Int J Rock Mech Min Sci* 46(1):200–209
- Feng CL, Wu XQ, Ding DX et al (2009) Investigation on fatigue characteristics of white sandstone under cyclic loading. *Chin J Rock Mech Eng* 28(S1):2749–2754
- Fuenkajorn K, Phueakphum D (2010) Effects of cyclic loading on mechanical properties of Maha Sarakham salt. *Eng Geol* 112(1–4):43–52
- Ge XR, Jiang Y, Lu YD et al (2003) Testing study on fatigue deformation law of rock under cyclic loading. *Chin J Rock Mech Eng* 22(10):1581–1585
- Hamid RN, Abdolhadi G (2014) Brittleness effect on rock fatigue damage evolution. *Rock Mech Rock Eng* 47(5):1839–1848
- He MM, Chen YS, Li N et al (2015) Deformation and energy characteristics of sandstone subjected to uniaxial cyclic loading. *J China Coal Soc* 40(8):1805–1812
- He MM, Li N, Chen YS et al (2016) Strength and fatigue properties of sandstone under dynamic cyclic loading. *Shock Vib* 2016:1–8
- Jiang DY, Fan JY, Chen J et al (2016) A mechanism of fatigue in salt under discontinuous cycle loading. *Int J Rock Mech Min Sci* 86:255–260
- Lazan BJ (1968) Damping of material and members in structural mechanics. Pergamon Press, London, pp 41–46
- Lu GM, Li YH (2016) Influence of confining pressure on fatigue deformation properties of yellow sandstone. *Rock Soil Mech* 37(7):1847–1856
- Lu GM, Li YH, Zang XW et al (2015) Fatigue deformation characteristics of yellow sandstone under cyclic loading. *Chin J Geotech Eng* 37(10):1886–1892
- Ma DP (2016) Basic experiment research of failure mechanism and precursory characteristics of rock under triaxial unloading confining pressure. Doctor of Philosophy from Shandong University of Science and Technology, Qingdao, pp. 59–61
- Wu MB (1982) The Effect of Loading Rate on the Compressive and Tensile Strength of Rocks. *Chin J Geotech Eng* 4(2):2610–2615
- Xiao JQ, Ding DX, Jiang FL et al (2010) Fatigue damage variable and evolution of rock subjected to cyclic loading. *Int J Rock Mech Min Sci* 47(3):461–468
- Yang YJ, Song Y, Chu J (2007) Experimental study on characteristics of strength and deformation of coal under cyclic loading. *Chin J Rock Mech Eng* 26(1):201–205
- Yin XT, Ge XR, Li CG et al (2010) Influences of Loading rates on Mechanical behaviors of Rock Materials. *Chin J Rock Mech Eng* 29(S1):2610–2615
- Zhang Y (2011) Experimental research on characteristics of deformation and dissipated energy of rock under cyclic loading conditions. Master of Philosophy from Chongqing University, Chongqing, pp 33–40
- Zhang QX, Ge XR, Hang M et al (2006) Testing study on fatigue deformation law of red-sandstone under triaxial compression with cyclic loading. *Chin J Rock Mech Eng* 25(3):473–478